Research Article

Received: 29 May 2014 Revised: 21 July 2014 Accepted article published: 31 July 2014 Published online in Wiley Online Library: 26 August 2014

(wileyonlinelibrary.com) DOI 10.1002/pi.4793

Electrospun crosslinked poly(acrylic acid) fiber constructs: towards a synthetic model of the cortical layer of nerve

Linghui Meng,[a,†] Wimonwan Klinkajon,[b] Prae-ravee K-hasuwan,[b] Shannon Harkin,[c,‡] Pitt Supaphol[b] and Gary E Wnek[a,*]

Abstract

In an attempt to mimic properties of the polyanionic nanofibrous cortical layer (ectoplasm) of nerve, tube-shaped poly(acrylic acid) (PAA) nanofiber constructs were prepared via electrospinning. The influence of processing parameters on the morphology of the electrospun PAA nanofibers was systematically investigated. Smooth and uniform PAA nanofibers with average fiber diameter of 820 nm were produced at a concentration of 4 wt% with a flow rate of 0.8 mL h^{-1} when a high voltage of 15 kV was applied. Water-stable PAA nanofibers were obtained by thermally crosslinking PAA with ethylene glycol. The resulting tubes were neutralized to the sodium polyacrylate form and were shown to undergo reversible and abrupt length changes upon titration with $CaCl_2$ followed by titration with sodium citrate. The sharpness of the length transition was found to be highly dependent upon the bathing NaCl concentration and the operation temperature. It is suggested that electrospun PAA may be a promising candidate as a key element of an abiotic macromolecular mimic of selected properties of axons.

Keywords: electrospinning; poly(acrylic acid); nanofiber; ectoplasm

INTRODUCTION

Previous studies have shown that a common underlying mechanism of cellular functions is a polymer gel phase transition, which means a major structural change is prompted by a subtle environmental change.[1,2] These phase transitions are thought to be involved in many cell behaviors, such as cellular solute exchange and transport, actin filament shortening, helix–coil transitions and several other force-dependent mechanisms.[3–5] Among them, an analogous phase transition in living nerve fibers has been extensively investigated in the last two decades.[6–12] The existence of cation-exchange processes involving Ca^{2+} and abrupt structural changes associated with these cation-exchange processes in the cortical layer of nerve fibers have been detailed in prior literature.[7,8] Tasaki and others have shown that the electrophysiological processes known as *nerve excitation and conduction* are basically manifestations of abrupt phase transitions of the cytoskeleton in the cortical gel layer of the axon and can be mimicked using synthetic polyanionic hydrogel monoliths.[9–12] Our attention has been piqued by such polyanionic hydrogels having been implicated in fundamental events associated with nervous transmission.

Electrospinning of micro- and nanofibers of natural and synthetic polymers has become an attractive approach as a processing platform for scaffolds for regenerative medicine and drug delivery.[13] Of particular interest has been the prospect of recapitulating the nanofibrous extracellular matrix which serves as the basic scaffold for the support of tissues and organs. We were attracted to the prospect of preparing synthetic polyanionic hydrogel nanofiber constructs to more closely mimic the cortical gel layer of nerve, which is known to be composed of actin-like nanofibers.[14] To that end, we report here a simple and reproducible process for fabricating tubular constructs of crosslinked electrospun poly(acrylic acid) (PAA). Our approach involves electrospinning of PAA from ethanol containing ethylene glycol (EG) and sulfuric acid followed by thermal treatment to promote esterification and crosslinking. Although the electrospinning of PAA has been reported previously,[13,15–19] we present here a new approach involving thermal post-crosslinking via entrained EG and what we believe to be the first demonstration of water-stable PAA nanofibrous tubes that exhibit reversible dimensional changes induced by monovalent–divalent cation exchange in aqueous solution.

* *Correspondence to: Gary E. Wnek, Department of Macromolecular Science and Engineering, Case Western Reserve University, Cleveland, OH 44106, USA. gew5@case.edu*

† *Present address: Harvard Apparatus Regenerative Technology, 84 October Hill Road, Holliston, MA 01746, USA*

‡ *Present address: Epic Systems, 1979 Milky Way, Verona, WI 53593, USA*

a *Department of Macromolecular Science and Engineering, Case Western Reserve University, Cleveland, OH 44106, USA*

b *Department of Biomedical Engineering and Master of Engineering and Management Program, Case Western Reserve University, Cleveland, OH 44106, USA*

c *Petroleum and Petrochemical College and Center for Petroleum, Petrochemicals, and Advanced Materials, Chulalongkorn University, Bangkok 10330, Thailand*

EXPERIMENTAL

Materials

PAA (average $M_v = 450\,000$ g mol^{-1}), EG (anhydrous), calcium chloride (anhydrous) and sodium citrate were purchased from Sigma-Aldrich and used without further purification. Poly(vinyl pyrrolidone) (PVP; $M_w = 360\,000$ g mol^{-1}) was purchased from Scientific Polymer Products, USA. Ethylenediaminetetraacetic acid (EDTA) disodium salt dehydrate, sodium hydroxide, sodium chloride, sulfuric acid, hydrochloric acid and water (HPLC grade) were purchased from Fischer Scientific and used as received.

Preparation of PAA ethanol solution

PAA solutions were prepared by dissolving the appropriate amount of polymer in ethanol with concentrations varied from 2 to 6 wt%. EG was added to each sample as a crosslinking agent with a concentration varying between 10 and 16 wt% relative to the PAA. Complete dissolution was observed after 24 h of mixing with a magnetic stir bar at ambient temperature. Sulfuric acid (1 mol L^{-1}) was added to the PAA–EG solution immediately before electrospinning processing at a concentration of 50 μL mL^{-1}.

Electrospinning of PAA nanofibers

PAA nanofibers were produced through a single-jet electrospinning technique. Typically, the experimental set-up consisted of a high-voltage power supply (0–30 kV; CZE1000R, Spellman High Voltage Electronics Corporation), a syringe pump (KD Scientific) and a variable-speed rotating stainless steel grounded mandrel (4.0 mm outer diameter × 15.0 cm length). In order to facilitate removal of electrospun PAA from the mandrel, a thin layer of PVP fibers was deposited by electrospinning a solution of 10 wt% PVP in ethanol prior to PAA electrospinning. PAA solutions were loaded into a 5 mL syringe with a blunt-tip 18-gauge needle (0.8 mm outer diameter) and placed 20 cm away from the leading face of the rotating collection target. The solutions were electrified by applying a positive voltage (15 kV) to the syringe needle by means of an alligator clamp. The solutions were transferred through syringe pumps with a mass flow rate from 0.8 mL h^{-1} to 1.0 mL h^{-1}. All experiments were carried out at room temperature and relative humidity of about 20%.

Thermal crosslinking of electrospun PAA fibrous tubes

Freshly made PAA nanofiber tubes were crosslinked on the mandrel via heat treatment in a vacuum oven at 130 °C and a reduced pressure of 25 in Hg (84.7 kPa) for 30 min, and then cooled to room temperature. We found that a thin coating of electrospun PVP allows more facile removal of the crosslinked PAA nanofibrous tubes from the mandrel after immersion in water as the PVP dissolves away.

Neutralization of PAA nanofibrous tubes

PAA nanofiber tubes, initially in the carboxylic acid form (PAA-H), were neutralized to the sodium carboxylate form (PAA-Na) by placing in 1 mol L^{-1} NaOH and 1 mol L^{-1} NaCl for approximately 1 h and then rinsing with water to remove residual salts. The masses of both dry and hydrated PAA-Na tubes were recorded using a balance (Mettler Toledo AL104).

Characterization of fiber morphology

The morphologies of electrospun PAA nanofibers were visualized by means of SEM. PAA samples were sputter-coated with an approximately 10 nm gold layer and observed using a JOEL JSM-6510LV SEM with an operating voltage of 15 kV. Fiber diameter analysis was done using free software ImageJ.

Morphological characterization was also performed using hydrated neutralized PAA tubes. For this purpose, small pieces of PAA samples were carefully cut in water and mounted on a standard SEM holder with the help of conductive carbon tapes. Then the samples were directly examined in an environmental SEM instrument (FEI Quanta 200 3D ESEM/FIB system) without sputter-coating. The operating voltage was 20 kV with a chamber pressure of 7.67 torr (1023 Pa).

Titrations of PAA tubes

Calcium chloride was selected to prepare an aqueous solution of Ca^{2+}. Length changes of PAA fibrous tubes were investigated by adjusting the concentration of Ca^{2+} through titration. Typically, in batch experiments, each neutralized PAA tube was placed in an Erlenmeyer flask with 50 mL of deionized (DI) water or water containing various concentrations of NaCl at room temperature. $CaCl_2$ solution (1 mol L^{-1}) was gradually added through a burette in aliquots of 0.5 mL each time. The length of the PAA tube was carefully measured using a ruler. The resulting shortened PAA-Ca tubes were withdrawn from the solution and rinsed with DI water.

In order to examine the reversibility of PAA tube dimensional changes, calcium chelators (EDTA or citrate) were utilized to remove Ca^{2+} from the PAA-Ca tubes. Briefly, EDTA or citrate solutions with a concentration of 0.2 mol L^{-1} were prepared by dissolving EDTA disodium dehydrate or sodium citrate separately in water. PAA-Ca tubes were immersed in 50 mL of DI water or water containing various concentrations of NaCl, and then were titrated with EDTA or citrate solution. The changes of tube length were carefully measured each time until they were constant in solution. The PAA-Na tubes were then withdrawn from the solutions and stored in DI water for future experiments. The titration experiments were repeated three times using three PAA tubes and the average percentages of changes in tube length were calculated.

Effect of temperature on tube length

Lightly crosslinked fibrous PAA tubes were prepared via the same procedure but with 10% EG related to PAA weight instead of 16%. The PAA tubes were neutralized to PAA-Na form, titrated to various extents with $CaCl_2$ up to and including the point of maximum contraction, and then immersed in 150 mmol L^{-1} NaCl. Tube lengths were then measured at 0, 25, 37, 45 and 55 °C.

RESULTS AND DISCUSSION

PAA nanofiber formation

In an attempt to optimize the electrospinning parameters, PAA–EG–ethanol solutions at a series of concentrations were prepared. All solutions produce a visually stable polymer jet but yield different fiber morphologies. Figures 1(a)–(c) show SEM images of electrospun PAA nanofibers at concentrations of 2, 4 and 6 wt% with a flow rate of 0.8 mL h^{-1} when an operating voltage of 15 kV is applied. It can be seen that, at a concentration of 2 wt%, some spindle-like structures form along the fibers. With an increase of the solution concentration, the spindle-like structures disappear. When the concentration is increased to 4 wt%, a fine fiber structure with an average diameter of 820 nm is clearly observed, as shown in Fig. 1(b). Further increasing the concentration leads to the formation of ribbon-like structures as

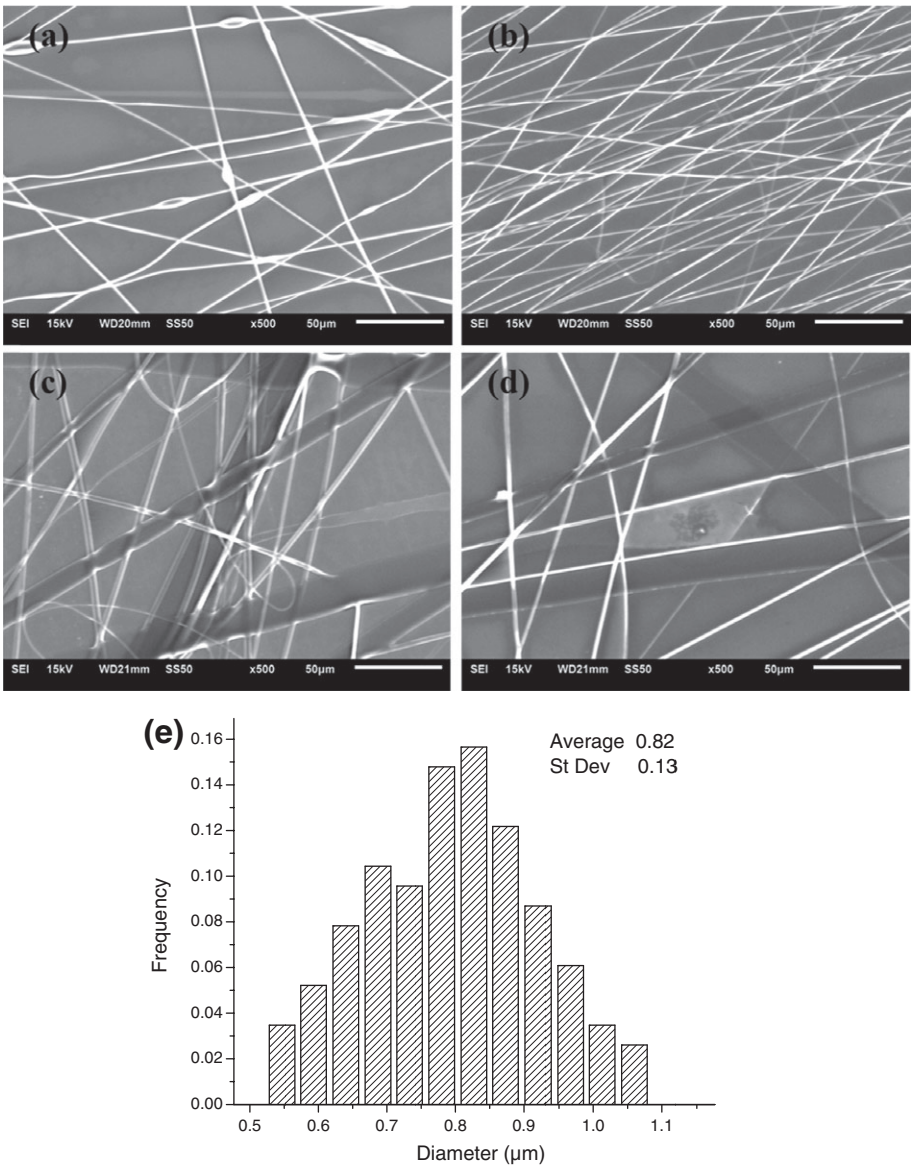

Figure 1. SEM images of PAA-H nanofibers electrospun from various concentrations at a flow rate of 0.8 mL h^{-1}: (a) 2 wt%, (b) 4 wt% and (c) 6 wt%; (d) 4 wt% at a flow rate of 1.0 mL h^{-1}. (e) Distribution of fiber diameter based on image (b).

well as thicker fibers, and distinct adhesion between the fibers appears to be dominant, resulting in a rough mat. It appears that the polymer concentration is one of the most critical parameters for controlling the quality of the nanofibers. The concentration is directly related to the viscosity, surface tension and conductivity of the polymer solution. Lower concentrations result in lower viscosity and higher surface tension, which favor the formation of bead structures, whereas increasing the concentration could result in increased solution viscosity, which is essential for the formation of fiber structures.

The flow rate of the polymer solution is another factor influencing the morphology of PAA nanofibers. When the PAA concentration is kept constant at 4 wt%, some ribbon-like fibers are formed with increasing flow rate from 0.8 to 1.0 mL h^{-1}, as shown in Fig. 1(d). This is because with very high flow rates fibers may not dry completely before reaching the collector, which leads to the formation of ribbon-like or flattened structures. In addition, it is worth noting that PAA nanofibers can be formed with a flow rate less than 0.8 mL h^{-1}, but in these cases the Taylor cone at the tip of the capillary cannot be maintained because the flow of solution through the capillary is insufficient to replace the solution ejected as the fiber jet.

Crosslinking of PAA nanofibers

Since PAA is water-soluble, crosslinking is necessary in order to retain the fiber structure of electrospun PAA. To that end, EG was found to be useful as a crosslinker, and was easily incorporated in the electrospun PAA fibers by addition to the electrospinning solutions. The resulting PAA-EG fibrous tubes were treated at 130 °C and 25 mmHg (3.3 kPa) for 30 min to form intermolecular crosslinks via ester formation between PAA and EG. A small amount of sulfuric acid was added to the electrospinning solution to catalyze the thermal esterification. The crosslinking reaction is idealized in Fig. 2, and it is likely that the material contains some fraction of 2-hydroxyethylacrylate units from reaction with only one hydroxyl group of EG.

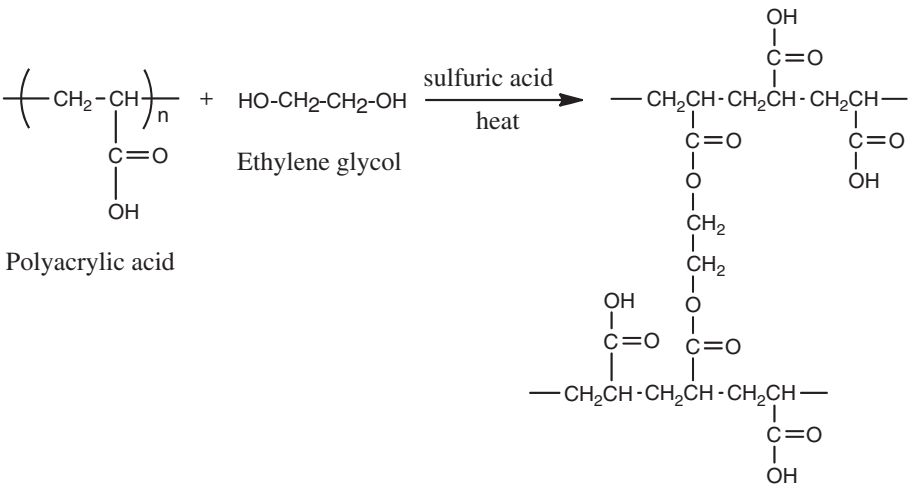

Figure 2. Thermal esterification of poly(acrylic acid) with ethylene glycol.

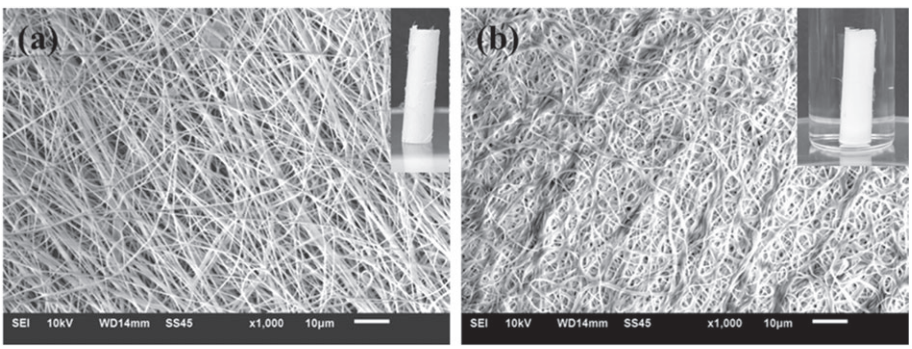

Figure 3. SEM images and snapshots (insets) of crosslinked PAA nanofiber tubes (a) before and (b) after immersing in water.

Stability testing of the thermally crosslinked PAA tubes was performed by soaking the samples in water for a week as shown in Fig. 3. No gross changes of tube dimensions (i.e. length and width) and loss of fiber morphology are noticeable, which indicates that sufficient crosslinks occur within the as-spun fibers.

Swelling behavior of PAA-H and PAA-Na tubes

The swelling ratio of PAA is determined from the relationship

$$\text{Swelling ratio} = \frac{W_s - W_0}{W_0}$$

where W_0 is the original weight of PAA and W_s is the weight of the sample immersed in solution for 1 h at room temperature and then tamped with a Kimwipe to remove excess water. Interestingly, the swelling ratio of the crosslinked PAA-H tubes is found to be 4.39 ± 0.14 in pure water. PAA-H tubes were converted to the sodium salt form (PAA-Na) by soaking the PAA-H tubes in a mixture of 1 mol L^{-1} NaOH and 1 mol L^{-1} NaCl solution. Figure 4 shows the wall thickness of crosslinked PAA tubes reversibly changing between about 3.85 mm and 0.75 mm for the PAA-Na and PAA-H tubes, respectively. The swelling ratio for PAA-Na tubes is 28.13 ± 1.23, while the swelling ratio for tubes in acid solution (1 mol L^{-1} HCl) is similar to that for the original PAA-H tubes obtained in pure water. It is worth noting that the lengths of the PAA tubes are essentially constant for both PAA-Na and PAA-H. This may be the result of preferential radial orientation of fibers during electrospinning on the rotating mandrel, affording tubular

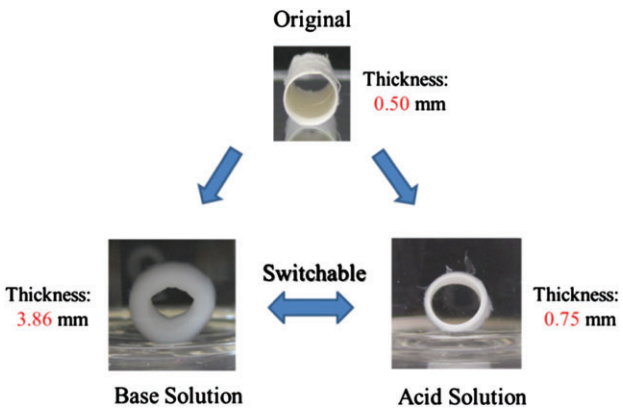

Figure 4. pH responsiveness of crosslinked PAA fiber tubes.

constructs in which PAA fiber swelling leads to macroscopic transverse (radial) rather than longitudinal swelling. A defined fibrous structure of hydrated PAA-Na tubes is observed using environmental SEM, as shown in Fig. 5.

Calcium ion titrations and chelation

Titration of a PAA-Na tube immersed in water with $CaCl_2$ leads to a distinct reduction in tube length as shown in Fig. 6(a). It can be seen that Ca^{2+} has little influence on the tube length initially. However, at about 20 mmol L^{-1} Ca^{2+}, there begins a decrease in tube length, and the contraction is completed in the range of

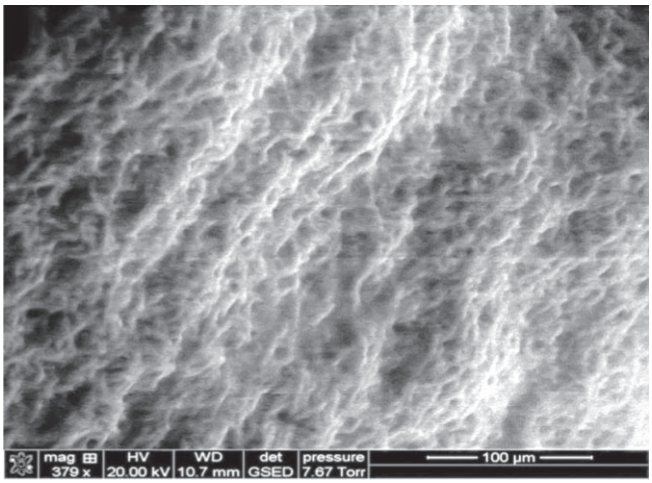

Figure 5. Typical environmental SEM image of neutralized PAA-Na fibers in water.

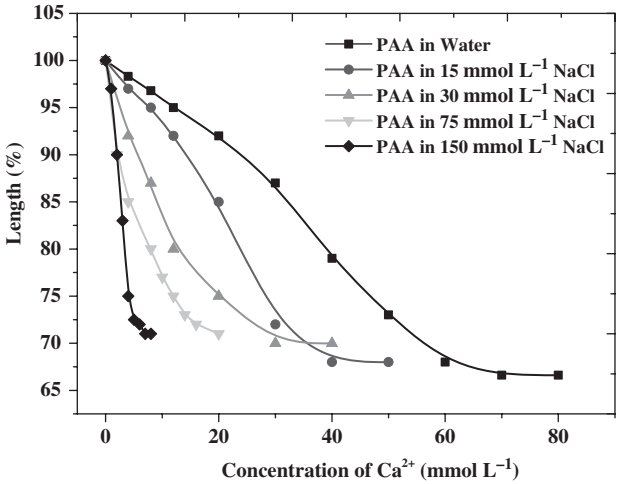

Figure 7. Length changes of PAA-Na nanofibrous tubes as a function of [Ca^{2+}] in solution with immersion in solutions of various concentrations of NaCl.

Ca^{2+} concentration just beyond about 55 mmol L^{-1}. As will be shown later, the tubes can be induced to return to their original dimensions upon treatment with the chelator sodium citrate.

The amount of water expulsion (deswelling) of PAA-Na fibrous tubes upon titration with $CaCl_2$ is calculated according to the following ratio:

$$\text{Deswelling} = \frac{W_{Ca}}{W_{Na}}$$

where W_{Na} is the weight of the PAA-Na tube and W_{Ca} is the weight of the PAA-Ca tube. The weight ratio is determined to be 0.16 ± 0.02, which suggests that a large amount of water is expelled due to the formation of cross-bridges between Ca^{2+} and COO^- groups of PAA. After calcium titration, the PAA-Na tubes decrease to about 65% of their original length, as shown in Fig. 6.

Further studies on the shrinking behavior of PAA-Na tubes with Ca^{2+} were carried out in NaCl aqueous solutions with the salt concentrations ranging from 15 to 150 mmol L^{-1} (Fig. 7). Of particular significance is the observation that contraction of PAA-Na tube length with increasing [Ca^{2+}] becomes sharper as the bathing NaCl concentration increases, eventually exhibiting a rather sharp transition, characteristic of a cooperative phenomenon, when the tube is immersed in 150 mmol L^{-1} NaCl during titration.

The addition of NaCl is expected to screen repulsive interactions between ionized (carboxylate) units in PAA-Na,[11] and indeed there was a small PAA-Na tube length contraction when immersed in NaCl solutions of increasing concentration. This can be seen in the trend of reducing maximum tube contractions (Fig. 7) with increasing NaCl concentration, resulting from slightly smaller initial lengths. Titration with Ca^{2+} causes contraction more readily with an increase of carboxylate screening, leading to an especially abrupt transition which may be thought of metaphorically as a 'zipper-like' mechanism.[20]

The PAA-Ca tubes can be re-expanded to their original lengths when titrated with sodium citrate, with the citrate concentrations needed for re-expansion depending on bathing NaCl concentration (Fig. 8), which closely mirrors the trends observed in Fig. 7. We also used disodium EDTA as a chelator but did not study this system in detail as we found that the length expansion of contracted

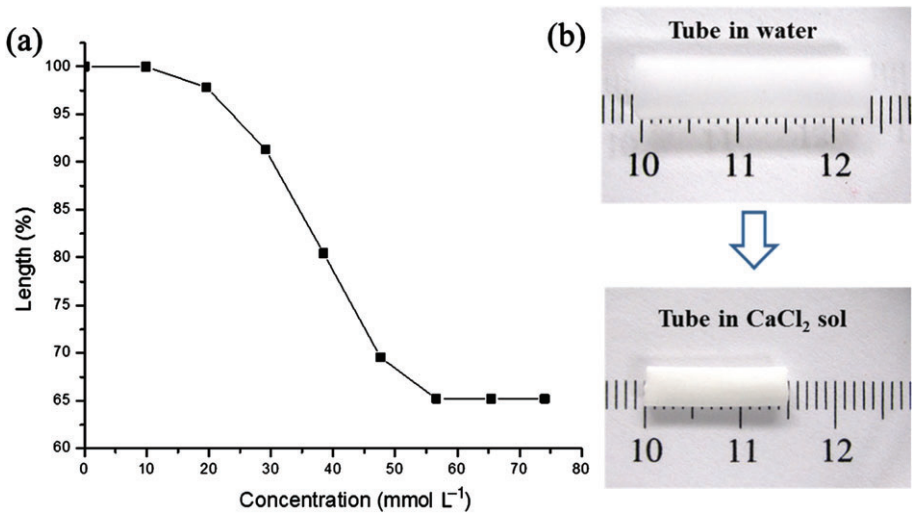

Figure 6. (a) Length changes of neutralized PAA-Na nanofibrous tubes with increasing [Ca^{2+}] in solution. (b) Snapshots of PAA-Na tubes at the beginning and the end of the titration.

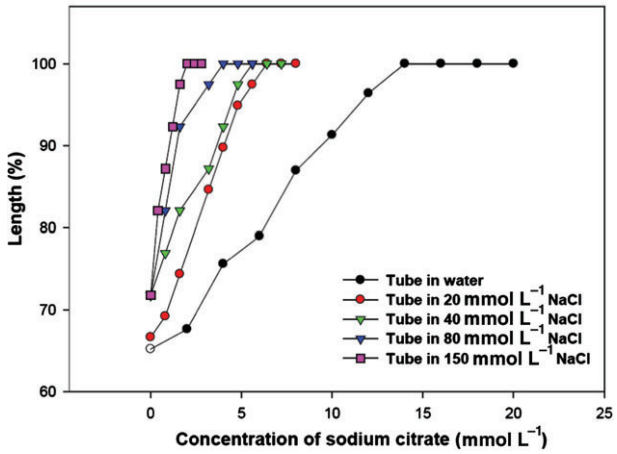

Figure 8. Length recovery of PAA-Ca nanofibrous tubes as a function of trisodium citrate concentration with immersion in solutions of various concentrations of NaCl.

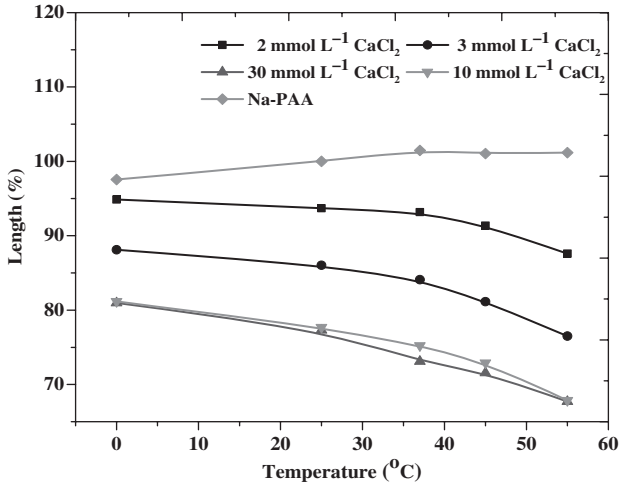

Figure 10. Length of PAA tubes initially in the sodium acrylate form and titrated with $CaCl_2$ in 150 mmol L^{-1} NaCl as a function of temperature of the aq. NaCl bath. Titrations were stopped at the concentrations shown.

tubes was rather slow compared with citrate. However, eventually full recovery was observed. Importantly, a fibrous porous structure was retained upon Ca^{2+}-induced contraction and re-expansion (in this case with disodium EDTA) as is evidenced by the SEM images in Fig. 9.

The fact that Ca^{2+}/Na^+ exchange leads to tube length changes whereas Na^+/H^+ exchange does not suggests that at least some Ca^{2+} binding occurs at fiber–fiber junctions, thus leading to measurable length changes.

Effect of temperature on length of PAA-Ca tubes immersed in 150 mmol L^{-1} NaCl

As pointed out by Tasaki,[21] studies on cation-exchange polymer resins reveal that exchange of Na^+ for Ca^{2+} is a weakly endothermic process,[22] and thus it is expected that Ca^{2+} will preferentially replace Na^+ as the temperature increases. It is therefore predicted that raising the temperature of a calcium ion-contracted PAA tube in NaCl of a given concentration will afford additional contraction, while cooling would lead to expansion. Figure 10 shows plots of tube length changes for a series of PAA-Na samples titrated in (and held in) 150 mmol L^{-1} NaCl with various amounts of Ca^{2+} (effectively marching through the sharp length reduction in Fig. 7) as a function of temperature from 0 to 55 °C, along with data for a PAA-Na tube in 150 mmol L^{-1} NaCl. In accord with the prediction above, all Ca^{2+}-treated tubes exhibit contraction with increasing temperature, with tubes titrated with the highest amounts of Ca^{2+} (10 and 30 mmol L^{-1}) showing the steepest dependences. In comparison, the PAA-Na sample exhibits a very small lengthening as temperature increases.

CONCLUSIONS

In this study, synthetic PAA nanofibers with average fiber diameter of 820 nm were produced by electrospinning of 4 wt% PAA ethanol solutions with a flow rate of 0.8 mL h^{-1}. PAA nanofibrous tubes were rendered water insoluble by heat-induced esterification and then neutralized to the sodium polyacrylate form in NaOH solution. It has been shown that neutralized PAA nanofibrous tubes can undergo reversible and abrupt structural changes with divalent–monovalent cation exchange and such changes became sharper with increasing NaCl concentration in solution. Moreover, the exchange of monovalent Na^+ with divalent Ca^{2+} was preferred as the operation temperature increased. These structural changes (shrinking and swelling) can be rather sharp and can be initiated and completed by a small change of Ca^{2+} or citrate concentration in solution, which suggests that these PAA fibrous tubular constructs may be promising candidates as a key element of an abiotic, macromolecular mimic of an axon. A more appropriate mimic of the cortical layer of nerve, or of active muscle, would be tubes or sheets of PAA fibers with a high degree of fiber orientation (longitudinal in the case of tubes[13]), and that is the subject of continuing research. Further studies focusing on understanding the details of the observations discussed here are in progress.

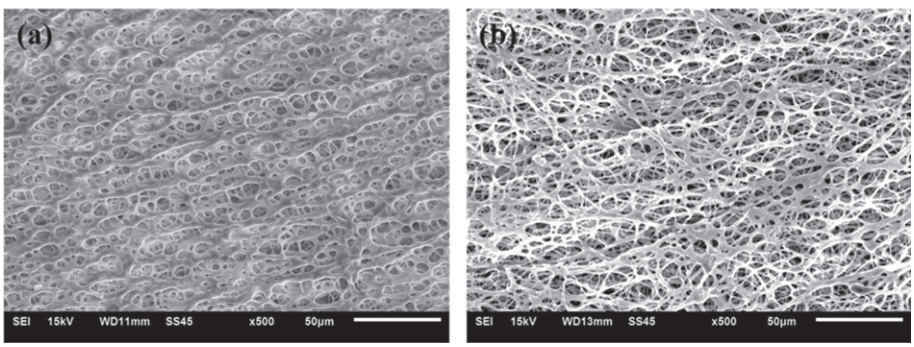

Figure 9. SEM images of PAA fiber network after (a) calcium titration and tube contraction and (b) disodium EDTA chelation.

ACKNOWLEDGEMENTS

We thank Dr John Layman of Procter and Gamble Co. who as an undergraduate at Virginia Commonwealth University developed initial formulations for PAA electrospinning and crosslinking. We are also grateful for support from the National Eye Institute of the National Institutes of Health (NIH), the Partnership For Innovation (PFI) Program of the National Science Foundation and the Petroleum and Petrochemical College of Chulalongkorn University.

REFERENCES

1 Tasaki I, *Ferroelectrics* **220**:305–316 (1999).
2 Trevors JT, Pollack GH, *Prog Biophys Mol Biol* **89**:1–8 (2005).
3 Pollack GH, *Adv Colloid Interface Sci* **103**:173–196 (2003).
4 Pollack GH *Jpn J Physiol* **51**:649–660 (2001).
5 Pollack GH, *J Mater Sci Mater Med* **13**:811–821 (2002).
6 Tasaki I, *Jpn J Physiol* **49**:125–138 (1999).
7 Tasaki I, *J Theor Biol* **218**:497–505 (2002).
8 Tasaki I, *J Theor Biol* **236**:2–11 (2005).
9 Tasaki I, On the reversible abrupt structural changes in nerve fibers underlying their excitation and conduction processes, in *Phase Transitions in Cell Biology*, ed. by Pollack GH and Chin W-C. Springer Science + Business Media, Amsterdam, pp. 1–21 (2008).
10 Tasaki I, *Physiology and Electrochemistry of Nerve Fibers*. Academic Press, New York, p. 257 (1982).
11 Horkay F, Tasaki I and Basser PJ, *Biomacromolecules* **2**:195–199 (2001).
12 Shklyar TF, Safronov AP, Klyuzhin IS, Pollack GH and Blyakhman FA, *Biophysics* **53**:544–549 (2008).
13 Huang C, Soenen SJ, Rejman J, Lucas B, Braeckmans K, Demeester J, *et al*, *Chem Soc Rev* **40**:2417–2434 (2011).
14 Metuzals J and Tasaki I, *J Cell Biol* **78**:597–621 (1978).
15 Jin X and Hsieh Y, *Polymer* **46**:5149–5160 (2005).
16 Xiao S, Shen M, Ma H, Guo R, Zhu M, Wang S *et al.*, *J Appl Polym Sci* **116**:2409–2417 (2010).
17 Kim B, Park H, Lee SH and Sigmund WM, *Mater Lett* **59**:829–832 (2005).
18 Li L and Hsieh Y, *Polymer* **46**:5133–5139 (2005).
19 Li L and Hsieh Y, *Nanotechnology* **16**:2852–2860 (2005).
20 Pollack GH, *Cell, Gels and the Engines of Life*. Ebner & Sons, Seattle, WA (2001).
21 Tasaki I, *Physiology and Electrochemistry of Nerve Fibers*. Academic Press, New York, p. 248 (1982).
22 Flett DS and Meares P, *Trans Faraday Soc* **62**:1469–1481 (1966).

